

THE USE OF MERIS FOR HARMFUL ALGAL BLOOM MONITORING IN THE SOUTHERN BENGUELA

S. Bernard ⁽¹⁾, C. Balt ⁽¹⁾, G. Pitcher ⁽²⁾, T. Probyn ⁽²⁾, A. Fawcett ⁽¹⁾ & A. Du Randt ⁽²⁾

(1) Department of Oceanography, University of Cape Town, Cape Town, South Africa.

(2) Marine & Coastal Management, Private Bag X2, Rogge Bay, Cape Town, South Africa

1. ABSTRACT

The southern Benguela suffers from the frequent occurrence of a variety of harmful algal blooms (HABs), often resulting in severe negative impacts to local marine ecosystems, communities and commercial marine concerns. The development of systems for the detection and monitoring of such blooms, using data from both the Medium Resolution Imaging Spectrometer (MERIS) and bio-optical moorings, are discussed. An experimental analytical reflectance inversion algorithm, allowing estimates of chlorophyll at high biomass and descriptors of algal size, is presented with application to MERIS data. The algorithm utilises equivalent size distributions of two layered spheres to describe the inherent optical properties of algal assemblages, thus allowing a description of reflectance data with regard to variables causal to algal optics; such as assemblage size and intracellular chlorophyll *a* concentration. The algorithm additionally allows the derivation of fluorescence line height and fluorescence quantum yield parameters. An important aspect of the work is the validation of MERIS water-leaving reflectance data and geophysical products in the high biomass and spatially heterogeneous waters associated with algal blooms. Initial validation studies using bio-optical data from automated buoy measurements and dedicated field campaigns are presented. Also discussed are the use of near real-time MERIS data from the Coastwatch programme for operational bloom detection, and the use of high spatial resolution FR data for the detection of small scale bloom events in the coastal environment.

2. INTRODUCTION

Harmful algal blooms (HABs) are a frequent occurrence in the Benguela system [1], often resulting in severe negative impacts to local marine ecosystems and communities, in addition to commercial marine concerns such as aquaculture operations. Harmful impacts of HABs, most often composed of a variety of dinoflagellate species, are associated with either the toxicity of some species present in the algal assemblage, or the high biomass such blooms can achieve. Collapse of high biomass blooms through natural causes such as nutrient exhaustion can lead to hypoxic events and in extreme cases, the production of hydrogen sulphide, frequently causing extensive mortalities of marine organisms. Effective ecosystem management requires a greater understanding of the variability of HABs as ecologically prominent phenomena, and the means of detecting and monitoring blooms in real time, through both *in situ* observation platforms and satellites. The MERIS sensor is particularly well suited to HAB applications, due to a combination of high spatial resolution, appropriately selected wavebands, and good radiometric sensitivity.

3. ALGORITHM DEVELOPMENT

3.1 Analytical Reflectance Algorithm Rationale

Conventional satellite-derived chlorophyll *a* products (Chl *a*) have become routine tools for the estimation of algal biomass in the sea. However, it has been demonstrated that bio-optical techniques can offer considerably more than simple algal biomass estimates, allowing the detection of changes in biomass-normalised algal optical properties and thus assemblage size and broad taxonomic identification [2, 3]. The provision of some form of assemblage description from ocean colour measurements offers significant advantages over simple biomass estimates. These include the detection of precursive and formative bloom conditions; an enhanced capacity to determine whether a bloom is of a potentially harmful nature; a better facility to monitor bloom growth, movement and decay; and a greater understanding of the bio-physical dynamics underlying bloom formation.

It is the absorbing and backscattering properties of the marine hydrosol that can be considered the most important inherent optical properties (IOPs) for ocean colour applications [4]. The ability to understand and characterise the absorbing and backscattering properties of the algal assemblage is thus central to the effective use of reflectance algorithms for HAB-related applications. It can be argued that ocean colour data are blind to the majority of morphological and genetic distinctions underlying conventional algal taxonomy; its effective use demands instead a metric based on the variables causal to the optical characteristics of the algal cell.

Mie modelling, and the related anomalous diffraction approximation, have played a central role in advancing the understanding of the processes underlying algal optical properties [5]. Algal absorption is well understood from this theoretical perspective, and is governed by three causal variables: the effective size of the algal cell or assemblage; the intracellular concentration of the pigments that are the predominant cellular absorbing material; and the spectral character of these pigments [2, 5]. Backscattering, the integrated angular scattering that is responsible for returning light to the surface of the sea, is considerably less well understood than absorption [6], but is nevertheless theoretically controlled, albeit in a less predictable manner, by the same causal variables as absorption: size and intracellular pigment configuration, with the additional influence of the material responsible for inducing changes to the real part of the cellular refractive index [5, 6]. However, whilst the absorption and total scattering of algal cultures have been successfully simulated using Mie theory [5], the few direct measurements made of algal angular scattering suggest that Mie theory is less well suited to describe backward scattering [6].

A necessary first step in the construction of more sophisticated reflectance models is thus the adoption of a modelling theorem that is capable of adequately simulating algal backscattering and other algal IOPs. The two-layered sphere appears to offer the simplest geometry capable of simulating the observed angular scattering of algal cells [7]. An algal IOP model, employing a two-layered geometry in conjunction with simply parameterised equivalent size distributions, is thus used to describe the absorption and backscattering properties of a hypothetical algal population [8]. This model is used as the core construct of an analytical reflectance inversion algorithm that allows the derivation of algal biomass (Chl *a*) and an algal size descriptor (effective diameter) from MERIS data, as described below

3.2 Analytical Reflectance Algorithm Structure

The reflectance approximation, commonly used for reflectance inversion algorithms [3, 4] expresses the light leaving the sea surface, i.e. the normalised water leaving reflectance $\rho_{norm}(\lambda)$, in terms of the absorption and backscattering properties of the upper optical depths:

$$\rho_{norm}(\lambda) = \pi \frac{f(\lambda) b_{bt}(\lambda)}{Q(\lambda) a_t(\lambda) + b_{bt}(\lambda)} \quad (1)$$

where $f/Q(\lambda)$ is a shape factor describing the angular structure of the light field [9], $a_t(\lambda)$ is the total absorption coefficient, and $b_{bt}(\lambda)$ is the total backscattering coefficient. The total absorption and backscattering coefficients are the summed total respective coefficients of the principal optical constituents of the water column: considered to be phytoplankton, coloured dissolved compounds here referred to as gelbstoff, particulate biological breakdown products otherwise known as detritus, other small particles generally considered to have a ubiquitous presence in the sea, such as lithogenic material or bacteria, and the seawater itself.

Whilst a full description of the algorithm structure is presented elsewhere [8], it can be summarised as follows. Inputs are MERIS atmospherically corrected multi-spectral normalised water leaving reflectance, on a pixel-by-pixel basis. The model uses seven solvable unknowns: chlorophyll *a* concentration (Chl *a*, mg m⁻³), algal effective diameter (d_{eff} , μm), the relative concentration of three representative algal groups, combined gelbstoff and detrital absorption (e.g. $a_{gd}(400)$, m⁻¹), and small particle backscattering (e.g. $b_{bs}(550)$, m⁻¹). Gelbstoff/detrital absorption and small particle backscattering employ constant spectral shapes and variable magnitude [8].

The algorithm employs a simplex solution method, using constant initial values, and is coded in Matlab R14. As the model specifically does not account for sun induced natural fluorescence [10], the convergence weighting for the Nelder-Mead solution is set to negligible values between 665 and 715 nm – the spectral region likely to be affected by natural algal fluorescence [*ibid.*]. The algorithm thus does not seek to match spectral reflectance values at these fluorescence wavelengths, and in effect offers a means of discriminating fluorescence effects, as have earlier models of a similar nature [3]. This allows the derivation of algal fluorescence quantum yield as an additional algorithm product [10], utilising integrated fluorescence (calculated from fitting a Gaussian distribution to modelled ρ_{norm} subtracted from measured ρ_{norm} at fluorescence wavebands), algal absorption as returned by the algorithm, and incident scalar irradiance calculated independently [11].

3.3 Analytical Reflectance Algorithm Performance

Fig.1 details the performance of the analytical reflectance algorithm with regard to inputs of hyperspectral and MERIS analogous multi-spectral reflectance data. Analyses shows that prediction of Chl *a* is sufficiently accurate for operational use over three decades of Chl *a* concentrations, whilst effective diameter and alloxanthin determinations should be used only for relative determinations of large scale assemblage changes.

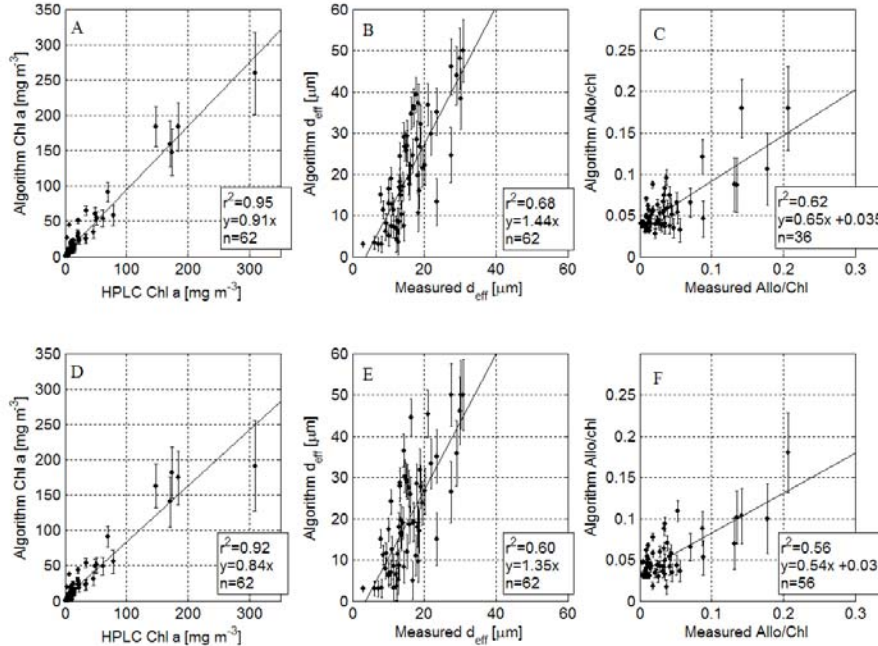


Fig.1. Analytical algorithm performance for hyperspectral reflectance (A,B,C) and MERIS waveband multi-spectral reflectance(D,E,F) derived from an independent data set of 62 in-water measurements of hyperspectral radiometric data, HPLC measured Chl *a* and relative alloxanthin ratio (used as a *Mesodinium rubrum* biomarker in this context), and Coulter Multisizer measured effective diameter.

3.4 The 709 algorithm – an empirical red wavelength Chl *a* algorithm

Whilst analytical reflectance algorithms are powerful in that they offer a solution based on first principles and an output of algal assemblage descriptors, they are expensive computationally. The two layered particle population simulations employed in the analytical reflectance algorithm have shown that algal backscattering exerts a relatively predictable effect on reflectance values at red wavelengths [8], typically seen as a distinctive peak in the reflectance spectrum at ~709 nm in high biomass blooms. This type of algorithm has the advantage of using a strong, direct signal (specifically

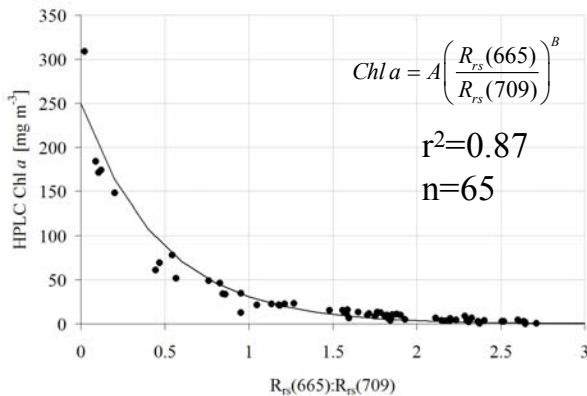


Fig. 3. Exponential best fit line for the $R_{rs}(665):R_{rs}(709)$ to Chl *a* relationship, using measured hyperspectral reflectance data and concomitant HPLC samples from a wide range of water types. Note that the use of a reflectance ratio allows analogous use regardless of the geometry used in different types of reflectance calculations

the ratio of the reflectance at 665 nm and 709 nm) in high biomass waters, unlike traditional empirical ocean colour algorithms, which suffer from vanishingly small signals at blue and green wavelengths in high biomass waters. Whilst considerable variability in the spectral shape of reflectance is introduced through variability in assemblage type, the presence of other backscattering constituents, and sun-induced fluorescence, it appears that the 665 to 709 nm reflectance ratio is strongly and relatively predictably influenced by algal biomass. This relationship can be quantified empirically (Fig. 3), and used in predictive application for Chl *a* calculations from both in-water and satellite derived reflectance measurements.

4. EXPERIMENTAL MERIS PRODUCTS

Application of the analytical reflectance algorithm described above to MERIS data has allowed derivation of chlorophyll, algal effective diameter and fluorescence synoptic products. These products have demonstrated their utility in several bloom situations, providing more accurate chlorophyll estimates at high biomass, and a biomass independent assemblage descriptor through algal size. Examples of analytical reflectance algorithm output can be seen in Fig. 4, demonstrating the utility of algorithm output for the analysis of mesoscale shelf processes. Two features in the imagery are of particular interest. The effective diameter data display an extensive feature of relatively high algal size, extending from the northern boundary of the Agulhas current, through the retroflexion zone and into the south Atlantic - closely following the thermal front visible in the SST imagery. Another feature of interest is the high fluorescence quantum yield values corresponding to active upwelling in the Namaqua cell.

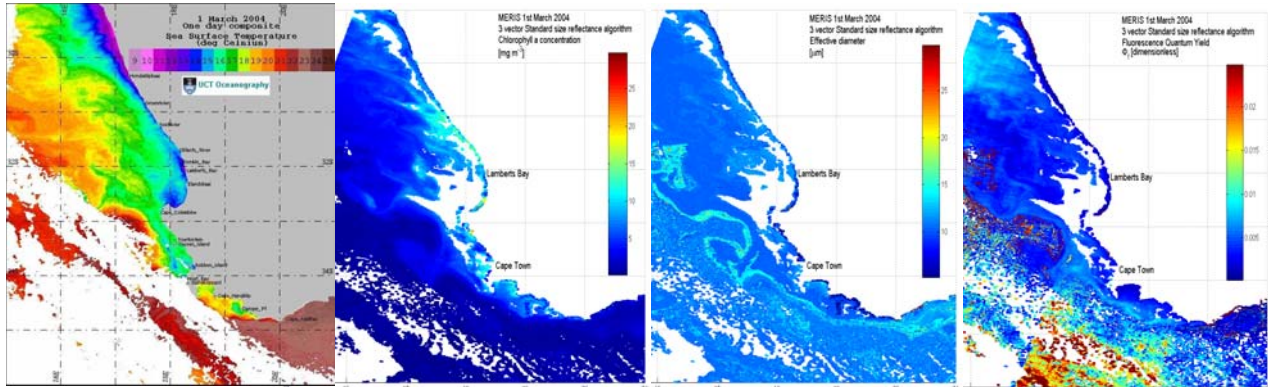


Fig. 4. NOAA SST and MERIS derived chlorophyll concentration, effective diameter and fluorescence quantum yield data from 1st March 2004. Note the feature corresponding to elevated effective diameter values in the thermal front extending from the northern boundary of the Agulhas current, through the retroflexion area and into the south Atlantic. Also note the dramatically elevated fluorescence quantum yield values corresponding to active upwelling at the northern boundary of the imagery.

5 COMPLEMENTARY BUOY SYSTEMS AND VALIDATION

Multi-sensor buoys offer high frequency Eulerian data relating to both the physics and biology of the Namaqua shelf system, in addition to offering reflectance validation data from paired radiometric sensors. The southern Namaqua shelf buoy is shown in Fig. 5, with sample validation data from a variety of water types in Fig. 6.



Fig. 5. The principal scientific (BOB) and marker buoys (BOMB) in position on the tight line mooring (left), and the upwelling radiance sensor arm on BOB (right). The scientific buoy has a payload of two Trios hyperspectral radiometers, a fluorometer, a thermistor chain, and an ADCP.

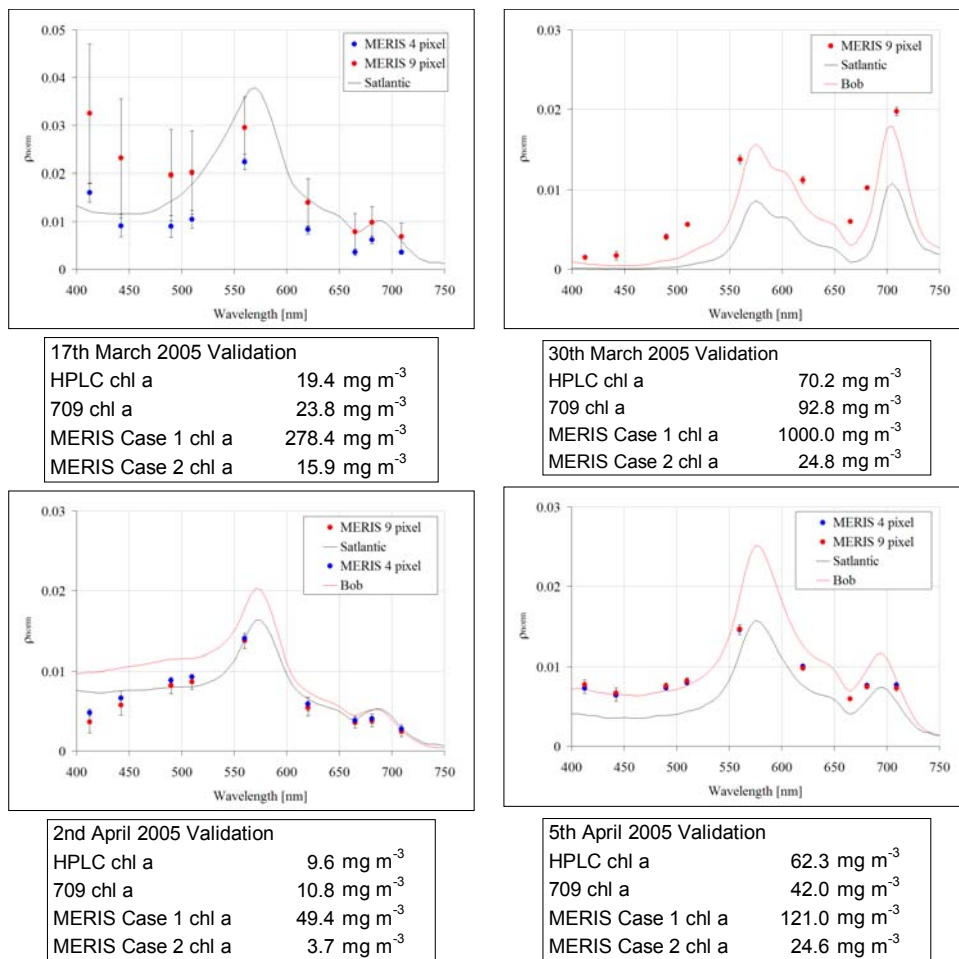


Fig. 6. Radiometric and HPLC measured chlorophyll a validation data for four samples from the Lamberts Bay region from the March/April 2005 field campaign. Graphed reflectance spectra are from the Satlantic H-TSRB (black lines), the Trios sensor pairing on BOB (red lines), a four pixel FR MERIS mean (blue dots) and a nine pixel FR MERIS mean (red dots). Remote sensing reflectance is generated from the in-water radiometer measurement using the previously discussed analytical reflectance algorithm to propagate upwelled radiance to the surface

6. EVENT SCALE BLOOM DETECTION

HAB focused observation systems are best demonstrated in a multi-sensor, multi-platform paradigm, allowing an appreciation of physical and biological variability from both Eulerian and synoptic perspectives. Several case studies of bloom events are presented here, over time scales of four to sixteen days. Fig. 7 shows an example of a dinoflagellate bloom impacting the coast, as measured by the BOB buoy and MERIS RR data, using the 709 nm algorithm. Fig. 8 shows the evolution of a multi-species bloom event over a two week period, using the 709 nm algorithm on MERIS FR data, and the effective diameter product from the analytical algorithm applied to MERIS RR data.

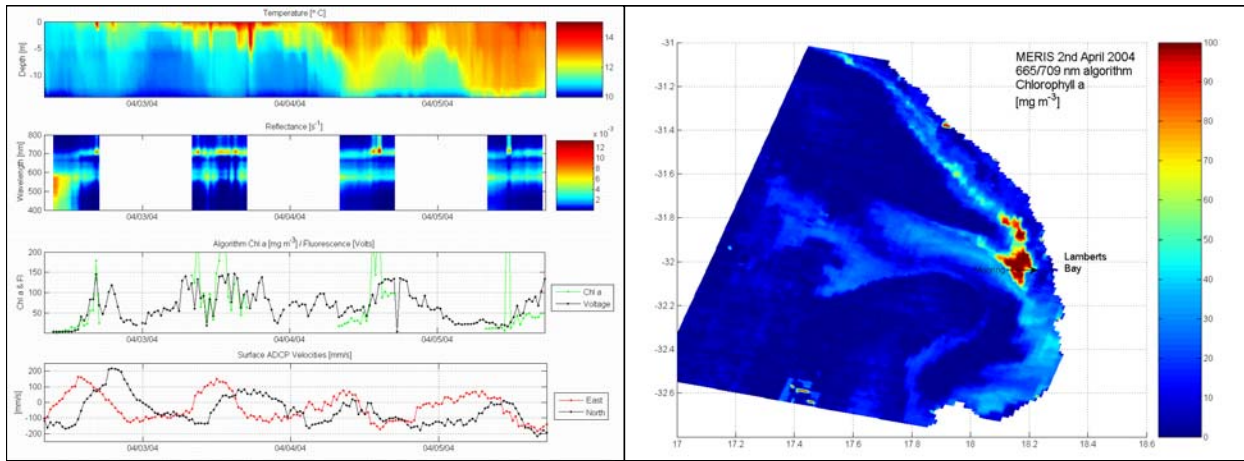


Fig.7. Mooring time series data and MERIS chlorophyll *a* data showing the detection and wide spatial extent of a bloom of the small dinoflagellate *Prorocentrum triestinum* from 2nd to 5th April 2004, in the Namaqua shelf region. The bloom appears at the mooring ~ 4 hours after the satellite overpass, as warm high biomass bloom waters are advected shorewards in the easterly surface flow. Satellite chlorophyll *a* data, derived through an experimental red band algorithm designed for high biomass application, show the widespread and complex distribution pattern of the bloom. Data such as these highlight the need for HAB real time observation systems to utilise both multi-sensor mooring and satellite derived data.

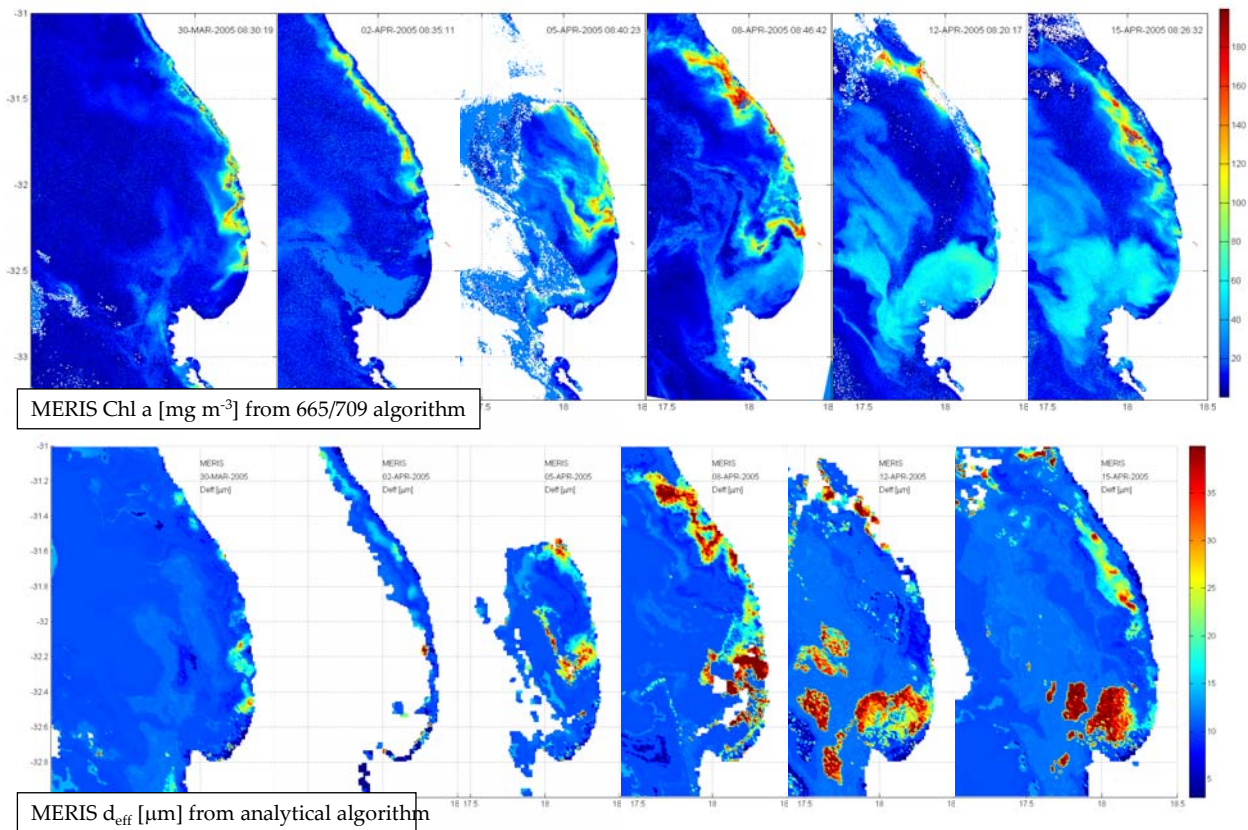


Fig. 8. An example of the utility of the different algorithm products in assessment of a multiple species bloom event April 2005 event on the Namaqua shelf. The effective diameter imagery before 5th April indicates the bloom is composed of small cells as confirmed by *in-situ* data showing dominance by the small dinoflagellate *Prorocentrum triestinum*. Effective diameter imagery after this time indicates a succession by large cells, in this case the large dinoflagellate *Ceratium furca*.

1. Pitcher, G. C., and D. Calder. Harmful algal blooms of the southern Benguela current: A review and appraisal of monitoring from 1989 to 1997. *S. Afr. J. mar. Sci.* 22: 255-271, 2000.
- 2 Bricaud, A., Claustre, H., Ras, J. and K. Oubelkheir. Natural variability of phytoplankton absorption in oceanic waters : influence of the size structure of algal populations. *J. Geophys. Res.*, 109, C11010. 2004.
3. Roesler, C.S., and E. J. Boss. Spectral beam attenuation coefficient retrieved from ocean colour inversion. *Geophys. Res. Lett.* 30(9), 1468-1471. 2003.
4. Morel, A. and L. Priour. Analysis of variations in ocean color, *Limnol. Oceanogr.*, 22: 709-722. 1977.
5. Morel A. and A. Bricaud. Inherent properties of algal cells including picoplankton: theoretical and experimental results. *Can. Bull. Fish. Aquat. Sci.*, 214: 521-559. 1986.
6. Stramski, D., E. Boss, D. Bogucki, and K. J. Voss. The role of seawater constituents in light backscattering in the ocean. *Progr. Oceanogr.*, 61: 27-56. 2004.
7. Quinby-Hunt, M.S., A.J. Hunt, K. Lofftus, and D. Shapiro. Polarized-light scattering studies of marine *Chlorella*. *Limnol. Oceanogr.*, 34 : 1587-1600. 1989.
8. Bernard, S. The Bio-Optical Detection of Harmful Algal Blooms. Ph.D thesis: University of Cape Town, 220pp. 2005.
9. Morel, A., D. Antoine, and B. Gentili. Bidirectional reflectance of oceanic waters: Accounting for Raman emission and varying particle phase function, *Appl. Opt.*, 41: 6289-6306. 2002.
- Morel, A. and B. Gentili. Radiation transport within oceanic (case 1) waters. *J. Geophys. Res.*, 109(C6): C06008. 2004.
10. Babin, M., Morel, A. and Gentili, B. Remote sensing of surface Sun-induced chlorophyll fluorescence: consequences of natural variations in the optical characteristics of phytoplankton and the quantum yield of chlorophyll a fluorescence. *Int. J. Rem. Sens.*, 17: 2417-2448. 1996.
- 11 Gregg W.W. and K.L. Carder. A simple spectral solar irradiance model for cloudless maritime atmospheres, *Limnol. Oceanogr.* 35,1657-1675. 1990.